ANZIAM J. **65** (2023), 55–78
doi:10.1017/S1446181123000172

WALL STABILIZATION IN MINES BY SPRAY-ON LINERS

D. P. MASON[1]✉, N. D. FOWKES[2], R. M. YEMATA[3], C. A. ONYEAGOZIRI[4] and H. YILMAZ[5]

(Received 28 December, 2022; accepted 30 March, 2023; first published online 31 August, 2023)

Abstract

Thin spray-on liners (TSLs) have been found to be effective for structurally supporting the walls of mining tunnels and thus reducing the occurrence of rock bursts, an effect primarily due to the penetration of cracks by the liner. Surface tension effects are thus important. However, TSLs are also used to simply stabilize rock surfaces, for example, to prevent rock fall, and in this context crack penetration is desirable but not necessary, and the tensile and shearing strength and adhesive properties of the liner determine its effectiveness. We examine the effectiveness of nonpenetrating TSLs in a global lined tunnel and in a local rock support context. In the tunnel context, we examine the effect of the liner on the stress distribution in a tunnel subjected to a geological or mining event. We show that the liner has little effect on stresses in the surrounding rock and that tensile stresses in the rock surface are transmitted across the liner, so that failure is likely to be due to liner rupture or detachment from the surface. In the local rock support context, loose rock movements are shown to be better achieved using a liner with small Young's modulus, but high rupture strength.

2020 *Mathematics subject classification*: primary 74B05; secondary 74A10.

Keywords and phrases: thin spray-on liners, tensile and shearing strength, stress concentration factor, cylindrical excavation.

1. Introduction

Shotcrete (concrete) has been used over the past 60 years [3] and possibly longer for mining tunnel strengthening; however, over the past 20 years thin (4 mm) spray-on liners (TSLs) have been used and have also been found to be effective for both

[1]School of Computational and Applied Mathematics, University of the Witwatersrand, Johannesburg, South Africa; e-mail: david.mason@wits.ac.za
[2]School of Mathematics and Statistics, University of Western Australia, Crawley, Western Australia, Australia; e-mail: neville.fowkes@uwa.edu.au
[3]African Institute for Mathematical Sciences, Muizenburg, Cape Town, South Africa; e-mail: reine.marquise@yahoo.fr
[4]University of Stellenbosch, Stellenbosch, South Africa; e-mail: assumpta@sun.ac.za
[5]Rock Mechanics Laboratory, CSIR, Johannesburg, South Africa; e-mail: halil.yilmaz.rml@gmail.com

protecting the miners from falling rock and reducing the occurrence of rock bursts and tunnel collapse. Evidently, the application of a spray to a tunnel wall is much simpler and cheaper than applying shotcrete to the wall, so that TSLs are much preferred provided they are effective. The support mechanism associated in the two cases is very different. Whereas shotcrete, being elastically strong, provides direct structural (arching) support, the elastically weak and thin TSLs cannot directly provide such support. The TSLs act by filling cracks in the rock face, and this effectively repairs the rock face by both preventing crack extension so that key rocks stay in place (Fowkes et al. [2]), and by increasing the hoop stress support in the filled surface layer of rock to that of the undamaged rock (Mason and Stacey [3]). However, mining engineers now use TSLs in a variety of mining environments which do not rely on the strengthening caused by crack penetration, although such penetration would be an added bonus. A case in point is the coating of a newly mined surface to stabilize it by preventing rock fall, thus enabling work to proceed unimpeded. In these (nonpenetration) applications the liners provide some resistance to the fracture failure caused by crack creation and extension, but in cases in which the rock is already fractured the liners act to prevent further dilation. In such contexts it is important to select the "right" TSL for the specific application and geological situation. The mechanical properties of the liner (elastic properties and tensile or shear strength) and the bonding strength of the liner on the rock surface are most important in this regard. Some end-users view tensile strength to be the most important property and the bonding to be an inferior one, while some others consider the bonding to be important also.

Stacey and Yu [5] and Tannant [6] identified various mechanisms for the action of TSLs, and discrete element models were used by Stacey [4] to simulate liner behaviour in tunnels. While such numerical work is useful in a particular context, it is not so useful for determining the effect of various liner and contact adhesion properties on the outcome. The analytical models developed here are more useful in this regard.

In Sections 2 and 3 the stress distribution in a TSL lined cylindrical tunnel due to the application of a tensile stress at infinity (associated with either a geological or mining event) is determined, with particular emphasis placed on the liner tensile strength and adhesion properties. In Section 4 the local rock support properties of the liner are examined; again the effects of elastic and tensile strength and bond strength on the outcome are determined. While the specific circumstances examined do not cover all possible circumstances of TSL use, it is felt that the situations considered are representative. We present conclusions in Section 5.

2. Cylindrical excavation with a liner in a tensile field

Consider a cylindrical tunnel in a rock mass to which a TSL has been applied. The tunnel is perturbed by a tensile stress T at infinity which models a seismic event or a disturbance due to a mining excavation. Cylindrical polar coordinates (r, θ, z) with origin at the centre of a cross-section of the tunnel are used with the z-axis along the axis of the tunnel. The tunnel has radius b and the rock mass is the region $b \leq r \leq \infty$.

https://doi.org/10.1017/S1446181123000172 Published online by Cambridge University Press

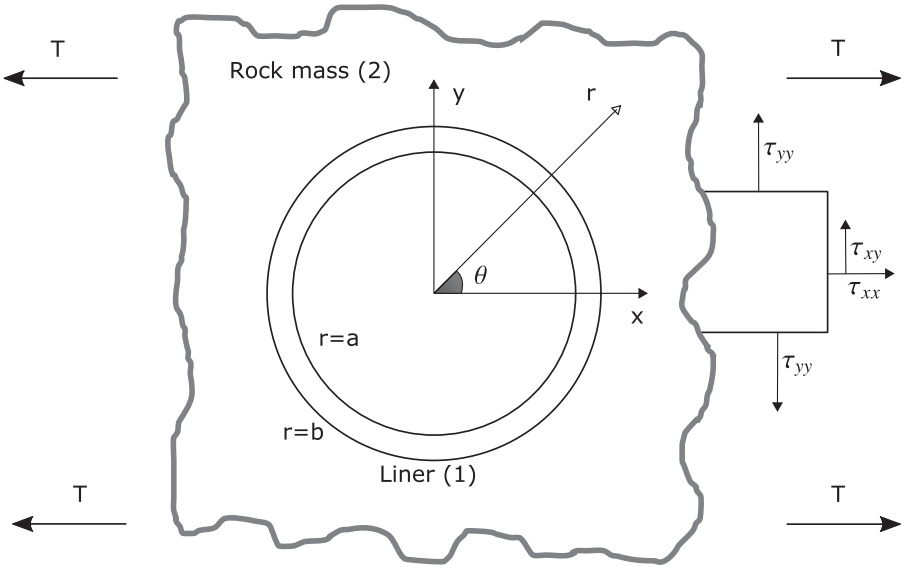

FIGURE 1. Cylindrical tunnel of radius b in an infinite elastic rock mass (region 2, $b \le r \le \infty$) with a spray-on liner (region 1, $a \le r \le b$) subjected to a uniform tensile stress T at infinity.

The TSL occupies the region $a \le r \le b$. It is assumed that the tunnel is sufficiently long that the plane strain theory of elasticity applies. All elastic variables are independent of z and there is no displacement in the z-direction. Quantities in the liner are denoted by a subscript or superscript 1, and quantities in the rock mass by a subscript or superscript 2. The tunnel and liner with the cylindrical polar and Cartesian coordinate systems are illustrated in Figure 1. We choose the perturbing tensile stress T to be in the x-direction because this will give the greatest hoop stress at $\theta = \pi/2$ and the rocks which are detached will fall under gravity.

In order to obtain the boundary condition as $r \to \infty$, consider the Cauchy stress tensor at large distances from the excavation expressed in Cartesian coordinates (x, y):

$$r \to \infty, \quad \tau_{xx}^{(2)} = T, \quad \tau_{xy}^{(2)} = 0, \quad \tau_{yy}^{(2)} = 0. \tag{2.1}$$

The Airy stress function $\phi(x, y)$ is defined by [1]

$$\tau_{xx} = \frac{\partial^2 \phi}{\partial y^2}, \quad \tau_{xy} = -\frac{\partial^2 \phi}{\partial x \partial y}, \quad \tau_{yy} = \frac{\partial^2 \phi}{\partial y^2}. \tag{2.2}$$

Solving (2.1) and (2.2) for the Airy stress function gives

$$r \to \infty : \quad \phi_2 = \tfrac{1}{2} T y^2 = \tfrac{1}{4} T r^2 (1 - \cos 2\theta),$$

where terms linear in x and y are dropped because they do not contribute to the stress tensor. The boundary condition as $r \to \infty$ is imposed on $\phi_2(r, \theta)$ because $\phi_2(r, \theta)$ is defined on the domain $b \le r \le \infty$.

https://doi.org/10.1017/S1446181123000172 Published online by Cambridge University Press

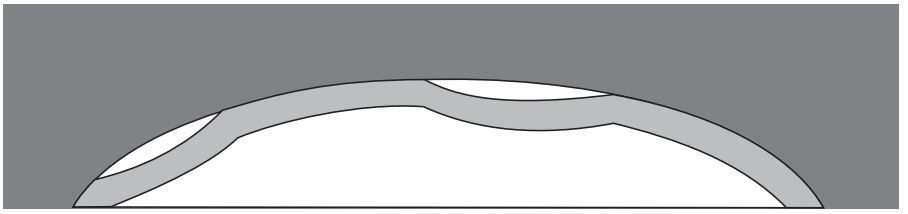

FIGURE 2. Weak bonding of the liner to the excavation.

The Airy stress functions, $\phi_1(r,\theta)$ and $\phi_2(r,\theta)$, satisfy the biharmonic equation:

$$a \le r \le b, \quad \nabla^4 \phi_1 = 0,$$
$$b \le r \le \infty, \quad \nabla^4 \phi_2 = 0,$$

where in cylindrical polar coordinates

$$\nabla^4 = \left(\frac{\partial^2}{\partial r^2} + \frac{1}{r}\frac{\partial}{\partial r} + \frac{1}{r^2}\frac{\partial^2}{\partial \theta^2} \right)^2.$$

The linear surface $r = a$ is traction-free. An aim of this investigation is to determine if the bonding of the TSL on the rock is a major contributing factor in stabilizing the surface of the tunnel. We therefore introduce a weak bonding factor λ $(0 \le \lambda \le 1)$ to model an excavation in which the liner is not in contact with the rock at all points of the surface, as illustrated in Figure 2. The radial and tangential components of the displacement vector are $u_r(r,\theta)$ and $u_\theta(r,\theta)$. The boundary conditions are

$$r = a: \quad \tau_{rr}^{(1)}(a,\theta) = 0, \tag{2.3}$$

$$r = a: \quad \tau_{r\theta}^{(1)}(a,\theta) = 0, \tag{2.4}$$

$$r = b: \quad \tau_{rr}^{(2)}(b,\theta) = \tau_{rr}^{(1)}(b,\theta), \tag{2.5}$$

$$r = b: \quad \tau_{r\theta}^{(2)}(b,\theta) = \lambda\, \tau_{r\theta}^{(1)}(b,\theta), \quad 0 \le \lambda \le 1, \tag{2.6}$$

$$r = b: \quad u_r^{(2)}(b,\theta) = u_r^{(1)}(b,\theta), \tag{2.7}$$

$$r = b: \quad u_\theta^{(2)}(b,\theta) = u_\theta^{(1)}(b,\theta), \tag{2.8}$$

$$r \to \infty: \quad \phi_2(r,\theta) = \frac{T}{4} r^2 - \frac{T}{4} r^2 \cos 2\theta. \tag{2.9}$$

A liner not firmly bonded to the rock mass is modelled in (2.6) by unequal tangential stress at the interface. One can think of the weak bonding factor λ as representing the ratio of the actual area of contact to the surface area of the rock at the interface. The boundary conditions (2.7) and (2.8) depend on the elastic constants through the inverse Hooke's law, and the stress will therefore depend on the elastic constants of the liner and rock mass.

https://doi.org/10.1017/S1446181123000172 Published online by Cambridge University Press

Guided by the boundary condition (2.9), we look for a solution in each region of the form

$$\phi(r,\theta) = f_0(r) + f_2(r)\cos\,2\theta. \tag{2.10}$$

Equation (2.10) satisfies the biharmonic equation provided

$$\frac{d^4f_0}{dr^4} + \frac{2}{r}\frac{d^3f_0}{dr^3} - \frac{1}{r^2}\frac{d^2f_0}{dr^2} + \frac{1}{r^3}\frac{df_0}{dr} = 0, \tag{2.11}$$

$$\frac{d^4f_2}{dr^4} + \frac{2}{r}\frac{d^3f_2}{dr^3} - \frac{9}{r^2}\frac{d^2f_2}{dr^2} + \frac{9}{r^3}\frac{df_2}{dr} = 0. \tag{2.12}$$

Equation (2.11) and (2.12) are both equidimensional (Euler) differential equations in r. We therefore look for solutions of the form

$$f(r) = A_n r^n, \tag{2.13}$$

where A_n is a constant. Equation (2.13) satisfies (2.11) provided $n = 0, 0, 2, 2$. Since $n = 0$ and $n = 2$ are repeated roots, the general solution of (2.11) is [1]

$$f_0(r) = A + Br^2 + C\ln\,r + Dr^2\ln\,r,$$

where A, B, C and D are constants. Equation (2.13) satisfies (2.12), provided $n = 4, 2, 0, -2$, and therefore the general solution of (2.12) is

$$f_2(r) = M\,r^4 + N\,r^2 + P + \frac{Q}{r^2},$$

where M, N, P and Q are constants. Hence,

$$\begin{aligned}\phi_s(r,\theta) = {} & A_s + B_s\,r^2 + C_s\ln r + D_s\,r^2\ln r \\ & + \left(M_s\,r^4 + N_s\,r^2 + P_s + \frac{Q_s}{r^2}\right)\cos\,2\theta, \quad s = 1, 2.\end{aligned}$$

Since the components of the Cauchy stress tensor are defined in terms of the derivatives of ϕ, we can take $A_1 = 0$ and $A_2 = 0$, while from the boundary condition (2.9) as $r \to \infty$,

$$B_2 = \frac{T}{4}, \quad D_2 = 0, \quad M_2 = 0, \quad N_2 = -\frac{T}{4}.$$

Hence,

$$\phi_1(r,\theta) = B_1r^2 + C_1\ln\,r + D_1r^2\ln\,r + \left(M_1r^4 + N_1r^2 + P_1 + \frac{Q_1}{r^2}\right)\cos 2\theta, \tag{2.14}$$

$$\phi_2(r,\theta) = \frac{T}{4}\,r^2 + C_2\ln\,r + \left(-\frac{T}{4}\,r^2 + P_2 + \frac{Q_2}{r^2}\right)\cos 2\theta. \tag{2.15}$$

Equations (2.14) and (2.15) contain 10 unknown constants which will be obtained from 10 algebraic equations derived from the boundary conditions.

https://doi.org/10.1017/S1446181123000172 Published online by Cambridge University Press

In order to impose the boundary conditions, it is first necessary to calculate the components of the Cauchy stress tensor which, in terms of the Airy stress function, are

$$\tau_{rr} = \frac{1}{r^2}\frac{\partial^2\phi}{\partial\theta^2} + \frac{1}{r}\frac{\partial\phi}{\partial r}, \tag{2.16}$$

$$\tau_{r\theta} = -\frac{\partial}{\partial r}\left(\frac{1}{r}\frac{\partial\phi}{\partial\theta}\right), \tag{2.17}$$

$$\tau_{\theta\theta} = \frac{\partial^2\phi}{\partial r^2}. \tag{2.18}$$

The equations of static equilibrium with zero body force are identically satisfied by (2.16)–(2.18). The components of the Cauchy stress tensor in the liner are

$$\tau^{(1)}_{rr}(r,\theta) = 2B_1 + D_1 + \frac{C_1}{r^2} + 2D_1\ln r + \left[-2N_1 - \frac{4P_1}{r^2} - \frac{6Q_1}{r^4}\right]\cos 2\theta, \tag{2.19}$$

$$\tau^{(1)}_{r\theta}(r,\theta) = \left[6M_1r^2 + 2N_1 - \frac{2P_1}{r^2} - \frac{6Q_1}{r^4}\right]\sin 2\theta, \tag{2.20}$$

$$\tau^{(1)}_{\theta\theta}(r,\theta) = 2B_1 + 3D_1 - \frac{C_1}{r^2} + 2D_1\ln r + \left[12M_1r^2 + 2N_1 + \frac{6Q_1}{r^4}\right]\cos 2\theta. \tag{2.21}$$

The components of the Cauchy stress tensor in the rock mass are obtained from (2.19)–(2.21) by setting

$$B_1 = \frac{T}{4}, \quad C_1 = C_2, \quad D_1 = 0, \quad M_1 = 0, \quad N_1 = -\frac{T}{4}, P_1 = P_2, \quad Q_1 = Q_2. \tag{2.22}$$

This gives

$$\begin{aligned}
\tau^{(2)}_{rr}(r,\theta) &= \frac{T}{2} + \frac{C_2}{r^2} + \left[\frac{T}{2} - \frac{4P_2}{r^2} - \frac{6Q_2}{r^4}\right]\cos 2\theta,\\
\tau^{(2)}_{r\theta}(r,\theta) &= \left[-\frac{T}{2} - \frac{2P_2}{r^2} - \frac{6Q_2}{r^4}\right]\sin 2\theta,\\
\tau^{(2)}_{\theta\theta}(r,\theta) &= \frac{T}{2} - \frac{C_2}{r^2} + \left[-\frac{T}{2} + \frac{6Q_2}{r^4}\right]\cos 2\theta.
\end{aligned} \tag{2.23}$$

The four boundary conditions for the stress tensor, (2.3)–(2.6), give two systems of linear algebraic equations for the 10 constants. The first system consists of two equations for the four constants B_1, C_1, D_1 and C_2:

$$2a^2B_1 + C_1 + a^2(1 + 2\ln a)D_1 = 0, \tag{2.24}$$

$$2b^2B_1 + C_1 + b^2(1 + 2\ln b)D_1 - C_2 = \frac{b^2}{2}T. \tag{2.25}$$

https://doi.org/10.1017/S1446181123000172 Published online by Cambridge University Press

The second system consists of four equations for the six constants M_1, N_1, P_1, Q_1, P_2 and Q_2:

$$a^4N_1 + 2a^2P_1 + 3Q_1 = 0, \tag{2.26}$$

$$3a^6M_1 + a^4N_1 - a^2P_1 - 3Q_1 = 0, \tag{2.27}$$

$$b^4N_1 + 2b^2P_1 + 3Q_1 - 2b^2P_2 - 3Q_2 = -\frac{b^4}{2}\,T, \tag{2.28}$$

$$3\lambda b^6M_1 + \lambda b^4N_1 - \lambda b^2P_1 - 3\lambda Q_1 + b^2P_2 + 3Q_2 = -\frac{b^4}{4}\,T. \tag{2.29}$$

Finally, consider the displacement boundary conditions (2.7) and (2.8). The components $u_r(r,\theta)$ and $u_\theta(r,\theta)$ of the displacement vector are calculated as follows. The inverse Hooke's law for plane strain is first applied to obtain the strain tensor e_{ik} in terms of the stress tensor τ_{ik}:

$$\mathrm{e}_{rr} = \frac{(1-\sigma^2)}{E}\,\tau_{rr} - \frac{\sigma(1+\sigma)}{E}\,\tau_{\theta\theta}, \tag{2.30}$$

$$\mathrm{e}_{r\theta} = \frac{(1+\sigma)}{E}\,\tau_{r\theta}, \tag{2.31}$$

$$\mathrm{e}_{\theta\theta} = \frac{(1-\sigma^2)}{E}\,\tau_{\theta\theta} - \frac{\sigma(1+\sigma)}{E}\,\tau_{rr}, \tag{2.32}$$

where E is Young's modulus and $\sigma\,(0 \le \sigma \le 1/2)$ is the Poisson ratio. But in cylindrical polar coordinates

$$\mathrm{e}_{rr} = \frac{\partial u_r}{\partial r}, \tag{2.33}$$

$$\mathrm{e}_{r\theta} = \frac{1}{2}\left(\frac{1}{r}\,\frac{\partial u_r}{\partial \theta} + \frac{\partial u_\theta}{\partial r} - \frac{u_\theta}{r}\right), \tag{2.34}$$

$$\mathrm{e}_{\theta\theta} = \frac{1}{r}\,\frac{\partial u_\theta}{\partial \theta} + \frac{u_r}{r}. \tag{2.35}$$

The system (2.33)–(2.35) consists of three first-order partial differential equations for the two unknowns, u_r and u_θ. The compatibility condition for this system is the biharmonic equation for the Airy stress function which will be satisfied because the stress tensor which will be used in the inverse Hooke's law is calculated from an Airy stress function.

Consider first the displacement components, u_r and u_θ, in the liner. We substitute (2.19)–(2.21) into the inverse Hooke's law (2.30)–(2.32), and then substitute the components of the strain tensor into (2.33)–(2.35). We obtain the following three first-order partial differential equations for u_r and u_θ:

https://doi.org/10.1017/S1446181123000172 Published online by Cambridge University Press

$$\frac{\partial u_r^{(1)}}{\partial r} = \frac{1+\sigma_1}{E_1}\Big[2(1-2\sigma_1)B_1 + \frac{C_1}{r^2} + (1-4\sigma_1)D_1 + 2(1-2\sigma_1)D_1 \ln r + \Big(-12\sigma_1 M_1 r^2 - 2N_1 - 4(1-\sigma_1)\frac{P_1}{r^2} - \frac{6Q_1}{r^4}\Big)\cos 2\theta\Big], \tag{2.36}$$

$$\frac{1}{r}\frac{\partial u_r^{(1)}}{\partial \theta} + \frac{\partial u_\theta^{(1)}}{\partial r} - \frac{u_\theta^{(1)}}{r} = \frac{1+\sigma_1}{E_1}\Big[12M_1 r^2 + 4N_1 - \frac{4P_1}{r^2} - \frac{12Q_1}{r^4}\Big]\sin 2\theta, \tag{2.37}$$

$$\frac{\partial u_\theta^{(1)}}{\partial \theta} + u_r^{(1)} = \frac{1+\sigma_1}{E_1}\Big[2(1-2\sigma_1)B_1 r - \frac{C_1}{r} + (3-4\sigma_1)D_1 r + 2(1-2\sigma_1)D_1 r \ln r + \Big(12(1-\sigma_1)M_1 r^3 + 2N_1 r + 4\sigma_1\frac{P_1}{r} + \frac{6Q_1}{r^3}\Big)\cos 2\theta\Big]. \tag{2.38}$$

We integrate (2.36) and (2.38) with respect to r and θ, which gives $u_r(r,\theta)$ and $u_\theta(r,\theta)$. They contain arbitrary functions of integration which are obtained by substituting u_r and u_θ into the remaining equation (2.37) and using separation of variables. This gives

$$u_r^{(1)}(r,\theta) = \frac{1+\sigma_1}{E_1}\Big[2(1-2\sigma_1)B_1 r - \frac{C_1}{r} - D_1 r + 2(1-2\sigma_1)D_1 r \ln r + \Big(-4\sigma_1 M_1 r^3 - 2N_1 r + 4(1-\sigma_1)\frac{P_1}{r} + \frac{2Q_1}{r^3}\Big)\cos 2\theta\Big] - F_1 \sin\theta + G_1 \cos\theta, \tag{2.39}$$

$$u_\theta^{(1)}(r,\theta) = \frac{1+\sigma_1}{E_1}\Big[4(1-\sigma_1)D_1 r\theta + \Big(2(3-2\sigma_1)M_1 r^3 + 2N_1 r - 2(1-2\sigma_1)\frac{P_1}{r} + \frac{2Q_1}{r^3}\Big)\sin 2\theta\Big] - F_1 \cos\theta - G_1 \sin\theta + H_1 r, \tag{2.40}$$

where F_1, G_1 and H_1 are constants. The displacement in the rock mass is obtained from (2.39) and (2.40) by using the transformation (2.22):

$$u_r^{(2)}(r,\theta) = \frac{1+\sigma_2}{E_2}\Big[(1-2\sigma_2)\frac{T}{2}r - \frac{C_2}{r} + \Big(\frac{T}{2}r + 4(1-\sigma_2)\frac{P_2}{r} + \frac{2Q_2}{r^3}\Big)\cos 2\theta\Big] - F_2 \sin\theta + G_2 \cos\theta, \tag{2.41}$$

$$u_\theta^{(2)}(r,\theta) = \frac{1+\sigma_2}{E_2}\Big[-\frac{T}{2}r - 2(1-\sigma_2)\frac{P_2}{r} + \frac{2Q_2}{r^3}\Big]\sin 2\theta - F_2 \cos\theta - G_2 \sin\theta + H_2 r, \tag{2.42}$$

where F_2, G_2 and H_2 are constants. For single-valued solutions for $u_\theta^{(1)}(r,\theta)$ it is necessary that

$$D_1 = 0. \tag{2.43}$$

https://doi.org/10.1017/S1446181123000172 Published online by Cambridge University Press

We now substitute (2.39)–(2.43) into the displacement boundary conditions (2.7) and (2.8). We obtain

$$2(1-2\sigma_1)b^2B_1 - C_1 + \left(\frac{1-\sigma_1}{1-\sigma_2}\right)\frac{E_1'}{E_2'}\,C_2 = \frac{1}{2}\,(1-2\sigma_2)\left(\frac{1-\sigma_1}{1-\sigma_2}\right)\frac{E_1'}{E_2'}\,b^2T, \tag{2.44}$$

$$\begin{aligned}2\sigma_1\,b^6M_1 + b^4N_1 - 2(1-\sigma_1)b^2P_1 - Q_1 + 2(1-\sigma_1)\,\frac{E_1'}{E_2'}\,b^2P_2 \\ + \left(\frac{1-\sigma_1}{1-\sigma_2}\right)\frac{E_1'}{E_2'}\,Q_2 = -\frac{1}{4}\left(\frac{1-\sigma_1}{1-\sigma_2}\right)\frac{E_1'}{E_2'}\,b^4T,\end{aligned} \tag{2.45}$$

$$\begin{aligned}(3-2\sigma_1)^6M_1 + b^4N_1 - (1-2\sigma_1)\,b^2P_1 + Q_1 + (1-2\sigma_2)\left(\frac{1-\sigma_1}{1-\sigma_2}\right)\frac{E_1'}{E_2'}b^2P_2 \\ - \left(\frac{1-\sigma_1}{1-\sigma_2}\right)\frac{E_1'}{E_2'}\,Q_2 = -\frac{1}{4}\left(\frac{1-\sigma_1}{1-\sigma_2}\right)\frac{E_1'}{E_2'}b^4T,\end{aligned} \tag{2.46}$$

and

$$F_1 = F_2 = F, \quad G_1 = G_2 = G, \quad H_1 = H_2 = H,$$

where the reduced elastic modulus E' is defined by

$$E' = \frac{E}{1-\sigma^2}.$$

We will see that the solution depends on the ratio E_1'/E_2' of the reduced elastic moduli.

Consider now the physical interpretation [1] of the displacement

$$\begin{aligned}u_r(r,\theta) &= -F\sin\theta + G\cos\theta,\\ u_\theta(r,\theta) &= -F\cos\theta - G\sin\theta + Hr,\end{aligned}$$

which occurs in (2.39) and (2.40). When written in Cartesian coordinates this displacement is

$$u_x(x,y) = G - Hy, \quad u_y(x,y) = -F + Hx,$$

which describes a rigid body translation of G and $-F$ in the x- and y-directions and a rigid body rotation H about the z-axis. We therefore take $F = G = H = 0$.

Since $D_1 = 0$, only nine constants remain to be determined. The nine linear algebraic equations for the nine constants split into two uncoupled systems. Equations (2.24) and (2.25) with $D_1 = 0$ and (2.44) form a system of three equations for the three unknown constants B_1, C_1 and C_2 which we will refer to as System A. System A can be written in matrix form as

$$EX = F, \tag{2.47}$$

https://doi.org/10.1017/S1446181123000172 Published online by Cambridge University Press

where

$$E = \begin{bmatrix} 2a^2 & 1 & 0 \\ 2b^2 & 1 & -1 \\ 2(1-2\sigma_1)b^2 & -1 & \left(\frac{1-\sigma_1}{1-\sigma_2}\right)\frac{E_1'}{E_2'} \end{bmatrix}$$

and

$$X = \begin{bmatrix} B_1 \\ C_1 \\ C_2 \end{bmatrix}, \quad F = \begin{bmatrix} 0 \\ \frac{1}{2}\, b^2 T \\ \frac{1}{2}\,(1-2\sigma_2)\left(\frac{1-\sigma_1}{1-\sigma_2}\right) b^2 T \end{bmatrix}. \tag{2.48}$$

Equations (2.26)–(2.29), (2.45) and (2.46) form a system of six equations for six unknown constants, M_1, N_1, P_1, Q_1, P_2 and Q_2 which we will refer to as System B. System B can be written in matrix form as

$$RY = S,$$

where

$$R = \begin{bmatrix} 0 & a^4 & 2a^2 & 3 & 0 & 0 \\ 3b^6 & a^4 & -a^2 & -3 & 0 & 0 \\ 0 & b^4 & 2b^2 & 3 & -2b^2 & -3 \\ 3\lambda b^6 & \lambda b^4 & -\lambda b^2 & -3\lambda & b^2 & 3 \\ 2\sigma_1 b^6 & b^4 & -2(1-\sigma_1)b^2 & -1 & 2(1-\sigma_1)\frac{E_1'}{E_2'}\, b^2 & \left(\frac{1-\sigma_1}{1-\sigma_2}\right)\frac{E_1'}{E_2'} \\ (3-2\sigma_1)b^6 & b^4 & -(1-2\sigma_1)b^2 & 1 & (1-2\sigma_2)\left(\frac{1-\sigma_1}{1-\sigma_2}\right)\frac{E_1'}{E_2'} b^2 & \left(\frac{1-\sigma_1}{1-\sigma_2}\right)\frac{E_1'}{E_2'} \end{bmatrix}$$

and

$$Y = \begin{bmatrix} M_1 \\ N_1 \\ P_1 \\ Q_1 \\ P_2 \\ Q_2 \end{bmatrix}, \quad S = -\frac{1}{4}\, b^4 T \begin{bmatrix} 0 \\ 0 \\ 1 \\ 1 \\ \left(\frac{1-\sigma_1}{1-\sigma_2}\right)\frac{E_1'}{E_2'} \\ \left(\frac{1-\sigma_1}{1-\sigma_2}\right)\frac{E_1'}{E_2'} \end{bmatrix}. \tag{2.49}$$

The exact solution of Systems A and B can be derived using Mathematica or a similar computer language. However, the results are not sufficiently simple to be

https://doi.org/10.1017/S1446181123000172 Published online by Cambridge University Press

useful for physical interpretation. A perturbation solution of Systems A and B will be performed in Section 3, the physical interpretation of which is more apparent.

3. Perturbation solution for the stress

Since the radius of the cylindrical excavation is $r = b$, we take for the perturbation parameter

$$\varepsilon = \frac{b-a}{b},$$

and therefore

$$a = b(1-\varepsilon). \tag{3.1}$$

If the radius of the tunnel is $b = 2\,\mathrm{m}$ and the thickness of the TSL is 10 mm, then $\varepsilon = 0.005$. We therefore need to derive the solution only to first order in ε.

The limit $\varepsilon = 0$ corresponds to no lining. The first-order correction describes the effect of the lining on the mine wall.

3.1. System A Consider first the system (2.47) and the perturbation expansion

$$\begin{aligned} B_1 &= B_{10} + \varepsilon B_{11} + \mathrm{O}(\varepsilon^2), \\ C_1 &= C_{10} + \varepsilon C_{11} + \mathrm{O}(\varepsilon^2), \\ C_2 &= C_{20} + \varepsilon C_{21} + \mathrm{O}(\varepsilon^2), \end{aligned}$$

as $\varepsilon \to 0$. System A at zero order in ε can be expressed in matrix form as

$$E_0 X_0 = F_0\,, \tag{3.2}$$

where

$$E_0 = \begin{bmatrix} 2b^2 & 1 & 0 \\ 2b^2 & 1 & -1 \\ 2(1-2\sigma_1)b^2 & -1 & \left(\dfrac{1-\sigma_1}{1-\sigma_2}\right)\dfrac{E_1'}{E_2'} \end{bmatrix} \tag{3.3}$$

and

$$X_0 = \begin{bmatrix} B_{10} \\ C_{10} \\ C_{20} \end{bmatrix}, \quad F_0 = F,$$

where F is given by (2.48). The system (3.2) can be solved either manually or by using Mathematica or a similar computer language. We find that

$$B_{10} = \frac{1}{4}\frac{E_1'}{E_2'}\,T, \quad C_{10} = -\frac{1}{2}\frac{E_1'}{E_2'}\,b^2 T, \quad C_{20} = -\frac{1}{2}\,b^2 T.$$

https://doi.org/10.1017/S1446181123000172 Published online by Cambridge University Press

System A at first order in ε written in matrix form is

$$E_0 X_1 = F_1, \tag{3.4}$$

where E_0 is given by (3.3) and

$$X_1 = \begin{bmatrix} B_{11} \\ C_{11} \\ C_{21} \end{bmatrix}, \quad F_1 = \begin{bmatrix} \dfrac{E_1'}{E_2'}\, b^2 T \\ 0 \\ 0 \end{bmatrix}.$$

The solution of (3.4) is readily obtained, because the inverse of the same matrix E_0 as for the zero-order system (3.2) has to be calculated. The solution is

$$B_{11} = \frac{1}{4}\left[\frac{1}{1-\sigma_1} - \frac{1}{1-\sigma_2}\,\frac{E_1'}{E_2'}\right]\frac{E_1'}{E_2'}\,T,$$

$$C_{11} = \frac{1}{2}\left[\frac{1-2\sigma_1}{1-\sigma_1} - \frac{1}{1-\sigma_2}\,\frac{E_1'}{E_2'}\right]\frac{E_1'}{E_2'}\,b^2 T,$$

$$C_{21} = \frac{E_1'}{E_2'}\,b^2 T.$$

3.2. System B Consider next System B and the perturbation expansion

$$M_1 = M_{10} + \varepsilon M_{11} + \mathrm{O}(\varepsilon^2),$$

$$N_1 = N_{10} + \varepsilon N_{11} + \mathrm{O}(\varepsilon^2),$$

$$P_1 = P_{10} + \varepsilon P_{11} + \mathrm{O}(\varepsilon^2),$$

$$Q_1 = Q_{10} + \varepsilon Q_{11} + \mathrm{O}(\varepsilon^2),$$

$$P_2 = P_{20} + \varepsilon P_{21} + \mathrm{O}(\varepsilon^2),$$

$$Q_2 = Q_{20} + \varepsilon Q_{21} + \mathrm{O}(\varepsilon^2),$$

as $\varepsilon \to 0$. System B at zero order in ε in matrix form is

$$R_0 Y_0 = S_0, \tag{3.5}$$

where

$$R_0 = \begin{bmatrix} 0 & b^4 & 2b^2 & 3 & 0 & 0 \\ 3b^b & b^4 & -b^2 & -3 & 0 & 0 \\ 0 & b^4 & 2b^2 & 3 & -2b^2 & -3 \\ 3\lambda b^6 & \lambda b^4 & -\lambda b^2 & -3\lambda & b^2 & 3 \\ 2\sigma_1 b^6 & b^4 & -2(1-\sigma_1)b^2 & -1 & 2(1-\sigma_1)\dfrac{E_1'}{E_2'}\,b^2 & \left(\dfrac{1-\sigma_1}{1-\sigma_2}\right)\dfrac{E_1'}{E_2'} \\ (3-2\sigma_1)b^6 & b^4 & -(1-2\sigma_1)b^2 & 1 & (1-2\sigma_2)\left(\dfrac{1-\sigma_1}{1-\sigma_2}\right)\dfrac{E_1'}{E_2'}\,b^2 & \left(\dfrac{1-\sigma_1}{1-\sigma_2}\right)\dfrac{E_1'}{E_2'} \end{bmatrix} \tag{3.6}$$

https://doi.org/10.1017/S1446181123000172 Published online by Cambridge University Press

and

$$Y_0 = \begin{bmatrix} M_{10} \\ N_{10} \\ P_{10} \\ Q_{10} \\ P_{20} \\ Q_{20} \end{bmatrix}, \quad S_0 = S,$$

where the matrix S is given by (2.49). The solution to zero order in ε is

$$\begin{aligned} &M_{10} = 0, && N_{10} = -\frac{1}{4}\frac{E_1'}{E_2'}\,T, && P_{10} = \frac{1}{2}\frac{E_1'}{E_2'}\,b^2T, \\ &Q_{10} = -\frac{1}{4}\frac{E_1'}{E_2'}\,b^4T, && P_{20} = \frac{1}{2}\,b^2T, && Q_{20} = -\frac{1}{4}\,b^2T. \end{aligned} \tag{3.7}$$

This solution is independent of the weak bounding factor λ. To understand why this is the case, we observe that λ occurs only in the boundary condition (2.6). But at zero order in ε, from (3.1), $a = b$ and the boundary condition (2.4) becomes

$$\tau_{r\theta}^{(1)}(b, \theta) = 0.$$

Hence the boundary condition (2.6) reduces to

$$\tau_{r\theta}^{(2)}(b, \theta) = 0,$$

which does not depend on λ. The parameter λ is therefore absent from System B at zero order in ε and its solution does not depend on the strength of the bonding at the interface.

System B to first order in ε in matrix form is

$$R_0 Y_1 = S_1,$$

where R_0 is given by (3.6) and

$$Y_1 = \begin{bmatrix} M_{11} \\ N_{11} \\ P_{11} \\ Q_{11} \\ P_{21} \\ Q_{21} \end{bmatrix}, \quad S_1 = \frac{E_1'}{E_2'}\,b^4T \begin{bmatrix} 1 \\ -2 \\ 0 \\ 0 \\ 0 \\ 0 \end{bmatrix}.$$

https://doi.org/10.1017/S1446181123000172 Published online by Cambridge University Press

The inverse of the same matrix R_0 as in the zero-order system (3.5) has to be evaluated. The solution to first order in ε is

$$M_{11} = -\frac{1}{12}\left[\frac{3}{1-\sigma_1} - \frac{2\lambda+1}{1-\sigma_2}\,\frac{E_1'}{E_2'}\right]\frac{E_1'}{E_2'}\,\frac{T}{b^2},$$

$$N_{11} = \frac{1}{2}\left[\frac{\sigma_1}{1-\sigma_1} - \frac{(2\lambda-1)\sigma_2+1-\lambda}{1-\sigma_2}\,\frac{E_1'}{E_2'}\right]\frac{E_1'}{E_2'}\,T,$$

$$P_{11} = -\frac{1}{4}\left[\frac{1}{1-\sigma_1} + \frac{(2\lambda-1)(3-4\sigma_2)}{1-\sigma_2}\,\frac{E_1'}{E_2'}\right]\frac{E_1'}{E_2'}\,b^2T,$$

$$Q_{11} = \frac{1}{2}\left[1 + \frac{5\lambda-2-3(2\lambda-1)\sigma_2}{3(1-\sigma_2)}\,\frac{E_1'}{E_2'}\right]\frac{E_1'}{E_2'}\,b^4T,$$

$$P_{21} = -(2\lambda-1)\,\frac{E_1'}{E_2'}\,b^2T,$$

$$Q_{21} = \frac{1}{3}\,(4\lambda-1)\,\frac{E_1'}{E_2'}\,b^4T.$$

The weak bonding factor λ first occurs in the components of the Cauchy stress tensor in the liner and rock mass at order ε and only in the coefficients of $\cos 2\theta$ and $\sin 2\theta$. The components of the stress tensor in the liner and rock mass depend on the Young's modulus only through the ratio E_1'/E_2' of the reduced elastic moduli. They also depend explicitly on the Poisson ratio in the liner and rock mass.

3.3. Stress in liner and rock mass to first order in ε We first investigate the contribution made by the TSL to the transfer of stress from the rock mass and the effect of weak bonding on this stress transfer. From (2.23) the hoop stress in the rock mass correct to order ε is

$$\tau_{\theta\theta}^{(2)}(r,\theta) = \frac{1}{2}\,T\left[1 + \left(1 - 2\varepsilon\,\frac{E_1'}{E_2'}\right)\left(\frac{b}{r}\right)^2 - \left(1 + 3\left(1 - \frac{4}{3}\,\varepsilon\,(4\lambda-1)\,\frac{E_1'}{E_2'}\right)\left(\frac{b}{r}\right)^4\right)\cos 2\theta\right]. \tag{3.8}$$

The hoop stress in the rock mass at the interface $r = b$ is

$$\tau_{\theta\theta}^{(2)}(b,\theta) = T\left[1 - \varepsilon\,\frac{E_1'}{E_2'} - 2\left(1 - \varepsilon(4\lambda-1)\,\frac{E_1'}{E_2'}\right)\cos 2\theta\right]. \tag{3.9}$$

The presence of the cylindrical excavation in the rock mass increases the hoop stress in the rock when the rock mass is subjected to tension. This is described by the stress concentration factor, K, which is defined as the ratio of the maximum tensile stress in

https://doi.org/10.1017/S1446181123000172 Published online by Cambridge University Press

the rock mass with the tunnel to the tensile stress in the rock mass without the tunnel. The hoop stress (3.8) is a maximum at $r = b$ and $\theta = \pi/2$:

$$\tau^{(2)}_{\theta\theta}\left(b, \frac{\pi}{2}\right) = 3T\left[1 - \frac{8}{3}\left(\lambda - \frac{1}{8}\right)\frac{E_1'}{E_2'}\,\varepsilon\right]. \tag{3.10}$$

The tensile stress in the absence of the tunnel is T. Thus,

$$K = 3\left[1 - \frac{8}{3}\left(\lambda - \frac{1}{8}\right)\frac{E_1'}{E_2'}\,\varepsilon\right].$$

When the liner is absent, $\varepsilon = 0$ and the stress concentration factor is 3. If $1/8 < \lambda \leq 1$, the effect of the liner is to decrease the stress concentration in the rock mass due to the transfer of stress from the rock to the liner. The weaker the bonding, the less the reduction of the stress in the rock. If $0 < \lambda < 1/8$ such that the bonding is very weak, the presence of the liner increases the stress concentration in the rock. However, since ε for a TSL is very small ($\varepsilon \simeq 0.005$), the stress concentration factor (3.10) shows that a TSL does not make a significant contribution to the reduction of stress in the rock mass.

Consider now the tensile stress in the liner which is given by (2.21). Because the tensile stress in the liner is important, we write it out in full, correct to first order in ε, to show its dependence on λ and on the elastic constants:

$$\begin{aligned}\tau^{(1)}_{\theta\theta}(r,\theta) = \frac{E_1'}{E_2'}\,T\Bigg[&\frac{1}{2} + \varepsilon B^*_{11} + \left(\frac{1}{2} + \varepsilon C^*_{11}\right)\left(\frac{b}{r}\right)^2 \\ &+ \left(\varepsilon M^*_{11}\left(\frac{r}{b}\right)^2 - \frac{1}{2} + \varepsilon N^*_{11} + \left(-\frac{3}{2} + \varepsilon Q^*_{11}\right)\left(\frac{b}{r}\right)^4\right)\cos 2\theta\Bigg],\end{aligned}$$

where

$$\begin{aligned}B^*_{11} &= \frac{1}{2}\left[\frac{1}{1-\sigma_1} - \frac{1}{1-\sigma_2}\,\frac{E_1'}{E_2'}\right], \\ C^*_{11} &= -\frac{1}{2}\left[\frac{1-2\sigma_1}{1-\sigma_1} + \frac{1}{1-\sigma_2}\,\frac{E_1'}{E_2'}\right], \\ M^*_{11} &= -\left[\frac{3}{1-\sigma_1} - \frac{12\lambda+1}{1-\sigma_2}\,\frac{E_1'}{E_2'}\right], \\ N^*_{11} &= \frac{\sigma_1}{1-\sigma_1} - \frac{(2\lambda-1)\sigma_2 + 1 - \lambda}{1-\sigma_2}\,\frac{E_1'}{E_2'}, \\ Q^*_{11} &= 3\left[1 + \frac{5\lambda - 2 - 3(2\lambda-1)\sigma_2}{3(1-\sigma_2)}\,\frac{E_1'}{E_2'}\right].\end{aligned}$$

The weak bonding parameter λ enters only at order ε in the coefficient of $\cos 2\theta$ and does not contribute significantly to the tension in the liner. The tensile stress in the liner at the interface $r = b$ correct to order ε is

https://doi.org/10.1017/S1446181123000172 Published online by Cambridge University Press

$$\tau_{\theta\theta}^{(1)}(b,\theta) = \frac{E_1'}{E_2'}\,T\Bigg[1+\varepsilon\Big(\frac{\sigma_1}{1-\sigma_1} - \frac{1}{1-\sigma_1}\,\frac{E_1'}{E_2'}\Big) - 2\Big\{1+\varepsilon\Big(\frac{\sigma_1}{1-\sigma_1} - \frac{4\lambda-1+2(1-2\lambda)\sigma_2}{1-\sigma_2}\,\frac{E_1'}{E_2'}\Big)\Big\}\cos 2\theta\Bigg], \tag{3.11}$$

and at $\theta = \pi/2$,

$$\tau_{\theta\theta}^{(1)}\Big(b,\frac{\pi}{2}\Big) = 3\frac{E_1'}{E_2'}\,T\Big[1+\varepsilon\Big(\frac{\sigma_1}{1-\sigma_1} - \frac{8\lambda-1+4(1-2\lambda)\sigma_2}{3(1-\sigma_2)}\,\frac{E_1'}{E_2'}\Big)\Big]. \tag{3.12}$$

A significant difference between (3.11) and (3.12) in the liner at the interface and (3.9) and (3.10) in the rock at the interface is the factor E_1'/E_2' at zero order in the liner. To prevent the build up of tensile stress in the liner the ratio E_1'/E_2' should be kept small by selecting a liner with suitably small reduced elastic modulus E_1'. The zero-order term in (3.11) and (3.12) does not depend on the weak bonding factor λ or on the thickness of the liner, the effects of which are first order in ε.

Finally, consider the shear stress at the interface $r = b$. Using (2.20), it can be verified that the shear stress in the liner at the interface correct to order ε is

$$\tau_{r\theta}^{(1)}(b,\theta) = -4\varepsilon\,\frac{E_1'}{E_2'}\,T\sin 2\theta,$$

which is independent of the weak bonding factor λ that will enter at order ε^2. Unlike the tensile stress, the shear stress is proportional to the thickness of the liner through ε and therefore is small in a TSL. From the boundary condition (2.6) the shear stress in the rock mass at the interface is

$$\tau_{r\theta}^{(2)}(b,\theta) = \lambda\tau_{r\theta}^{(1)}(b,\theta) = -4\,\varepsilon\,\lambda\,\frac{E_1'}{E_2'}\,T\sin 2\theta.$$

The liner can fail under tension, *not* under shear, because the shear stress in the liner is small, of order ε. Slip or debonding between the liner and the rock will reduce tension in the liner and prevent liner failure under tension.

The shear and tensile stress in the liner and rock mass depend on the ratio E_1'/E_2' of the reduced elastic moduli. Typical numerical values for the elastic constants are

$$E_1 = 6\,GPa, \quad \sigma_1 = 0.3, \quad E_2 = 40\,GPa, \quad \sigma_2 = 0.25,$$

which gives for the ratio

$$\frac{E_1'}{E_2'} \simeq 0.15.$$

The effect of the liner on the stress distribution in the rock mass surrounding the tunnel is small and is little influenced by the boundary conditions. This is very different from the effect of penetration of liner material into cracks and fractures in the rock

https://doi.org/10.1017/S1446181123000172 Published online by Cambridge University Press

mass [2, 3]. The effect of the tunnel on the liner tensile stress is large, at zero order, through the ratio E_1'/E_2' of the reduced elastic moduli. This can cause the liner to detach.

4. Local rock support due to a TSL

Here we are concerned with the effectiveness of TSLs for restraining the movement of "loose" rocks on a wall surface, which may correspond to a tunnel wall. In the tunnel case considered in Sections 2 and 3 the liner may rupture under tension or may detach from the surface of the rock due to excessive shear across the adhesive layer. Such a separation of liner from the rock face will occur at isolated locations on the tunnel wall where the adhesion is weak (perhaps due to loose sand) or due to local protuberances.

While our focus is on "local restraint" issues, it must be kept in mind that if displaced rocks are key components for the structure then global collapse may occur, so such geometric issues necessarily play a role. Depending on the stability of the global structure and the local geological and mining forcing, one can decide to either strongly restrict the movement of loose rocks relative to the wall, thus strongly constraining the geometry, or weakly constrain the geometry. In this context, we have the following.

- Shotcrete can provide strong "structural" support. This strong resistance to movement, however, will result in large stresses if there is significant external forcing, and if rupture occurs then it is likely to be dramatic because of the large elastic energy build-up in the shotcrete before rupture.
- At the other end of the spectrum we have steel meshes (with supporting bolts) which simply capture falling rocks; there is almost no strong structural support.
- The TSL liners are "elastically weak" but "lightly" constrain small movement (unless there is liner penetration). If, however, the liner detaches then rocks may be "basketed" by the liner, but less weakly than if mesh is used.

Figure 4 displays laboratory results for pull tests for various support types [6]. Note that steel reinforced shotcrete strongly resists movement until rupture. If weaker mesh reinforcement is used with shotcrete then again there is strong resistance to small movements but greater displacements can occur without rupture. A bolted wire mesh provides no resistance to wall movement until the mesh is fully stretched. Ideally, as displayed, one would like the liner to strongly resist movement but again allow larger displacements to occur without "collapse", as displayed in the ideal load–displacement curve. In practice, one might expect a load–displacement response for TSLs of the "generic type" shown. Here the liner provides moderate resistance to loading up until a limit $L^{\max}$ is reached, and then responds to additional loading by stretching a distance $d^{\max}$ before collapsing; the TSL thus accomplishes the desirable attributes of both shotcrete and bolted wire mesh. In a particular mining and geological context $L^{\max}$ and $d^{\max}$ may be prescribed so as to ensure structural stability, and the aim is to identify or design the TSL that realizes these values. The required elastic and adhesive parameters to achieve this behaviour may be obtained by changing the thickness of the liner or

https://doi.org/10.1017/S1446181123000172 Published online by Cambridge University Press

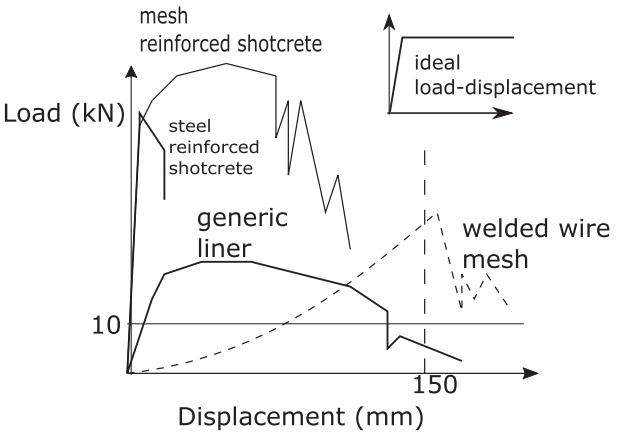

FIGURE 3. Load versus displacement (pull test) curves for various wall support procedures, including a generic TSL liner. An ideal load–displacement curve is also indicated. (Taken from [6].)

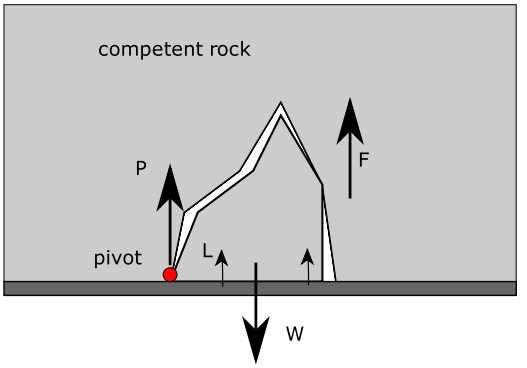

FIGURE 4. The rock tilts and remains in place due to the liner.

adjusting the chemical composition of the liner or adhesive. Loading–displacement curves of this nonlinear type are typical of rubber materials, so that it may be possible to simply design the TSL liner without consideration of the adhesive, but it seems more likely that adjustment of the adhesive properties will be necessary.

4.1. Support mechanisms and failure We will now examine various typical situations involving the use of liner support in mining. This work closely follows the work of Tannant [6].

Figure 4 shows a loose rock that remains in place on the roof of the tunnel because of liner constraint. This situation would arise if the rock split off from the wall after the liner was applied; in such a case there would be no penetration of the liner into wall cracks. Note in this case that the loose rock is partially supported by the competent

https://doi.org/10.1017/S1446181123000172 Published online by Cambridge University Press

FIGURE 5. Failure through liner rupture. Left: The supported rock. Right: A close up of the situation near the rupture point (circle). Two liner rupture modes are possible: shear failure and tensile failure.

TABLE 1. Polyurethane liner properties.

Young's modulus	E = 69–690 MPa
Tensile strength	τ_l = 8 MPa
Adhesive strength	τ_b = 1 MPa
Maximum strain	$e = 10^{-1}$
Bond width	w_b = 5 mm
Liner thickness	w_l = 4 mm

wall and partially supported by the liner. If the rock is sufficiently large the liner will not tightly restrain it and it will break loose.

One possible scenario is that the liner will fail either through shear rupture or through diagonal tensile rupture, as depicted in Figure 5 (right). Tannant noted that crude estimates of the size of rock that can be supported can be simply obtained by determining the force required to pull the loose bonded rock from the competent rock which is given approximately by

$$F = \tau_l w_l L$$

where τ_l (N/m) is the shear strength of the TSL and w_l is its thickness, and L the length of the crack separating the rock from the surface of the wall. Using Tannant's data for a w_l = 4 mm polyurethane liner (Table 1), and using a rock density of 2600 kg/m^3, this gives a prediction that a square rock of size 1 × 1 m and depth 0.5 m would be supported by a 4 mm TSL liner before rupture. Similar results are obtained if tensile rupture occurs. These results are *much* larger than one would expect, which suggests that the liner itself is unlikely to fail by this type of rupture. It seems more likely that the liner would tear. Laboratory and field observations suggest that this is the case [6].

The implication of the above is that liner rupture is very unlikely to be the failure mechanism; adhesive detachment from the wall is likely to occur before stress levels in the liner are sufficient to cause rupture, which is consistent with the results for polyurethane presented in Table 1; the bonding strength of the liner is much less than the shear and tensile strength T.

The liner acts as a membrane which exerts a tension force on the suspended rock. Under the action of an increasing expulsion force (in this case an increasing

https://doi.org/10.1017/S1446181123000172 Published online by Cambridge University Press

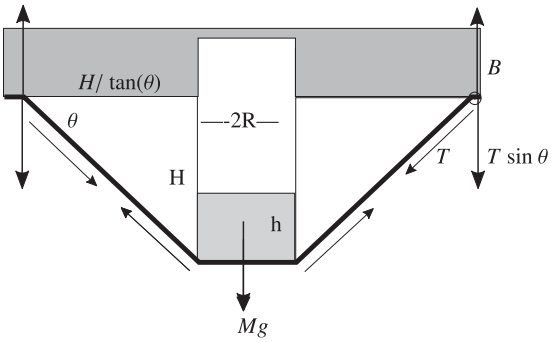

FIGURE 6. Cylindrical rock support geometry. Note that along the line of attachment (see circle) we have $B = T \sin\theta$.

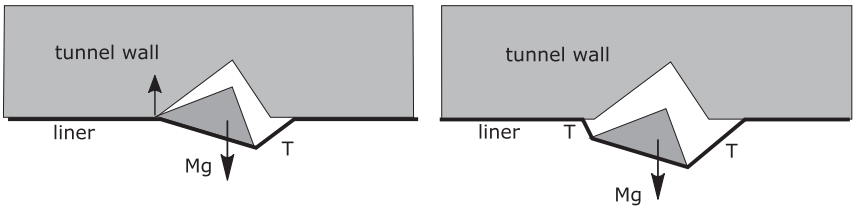

FIGURE 7. Attached and unattached rock held in place by a liner.

rock weight) liner/rock adhesive loss will first occur at some location around the perimeter of the wall crack separating the rock from the wall, and the liner will tear away from the crack and wall face while the normal component of the tensile force in the liner membrane exceeds the bonding force B (N/m), as shown in Figure 6. This process will cease when the forces are in balance so that

$$B = T \sin\theta, \tag{4.1}$$

where

$$B = \tau_b w_b, \quad T = \tau_l w_l, \tag{4.2}$$

and $w_b \approx w_l$ is the bond width. This result determines the equilibrium angle of attachment θ in terms of the bonding strength and local liner tension. During the detachment process the suspended loose rock will descend and rotate until the rock is fully supported with the net force and torque acting on the rock in balance, and with the attachment condition (4.2) being satisfied around the contact boundary. The rock may be partially supported by the wall or may be fully supported as depicted in Figure 7.

https://doi.org/10.1017/S1446181123000172 Published online by Cambridge University Press

Figure 6 displays a symmetric case in which a cylindrical rock of height h and radius R detaches from the wall. In this case the force balance for the rock requires

$$2\pi\left[R + \frac{H}{\tan\theta}\right]B = Mg, \tag{4.3}$$

and the tension in the liner is uniform around the (cylindrical) line of attachment. Torque balance is ensured by symmetry.

Assuming the liner remains bonded to the exposed face of the rock (the most likely scenario) the extension of the liner (change in length of the liner per unit initial length) is, from Figure 6, given by

$$e = \frac{1}{\cos\theta} - 1, \tag{4.4}$$

and, assuming a Young's law behaviour, we have, since $\tau_\ell = E(S\ell/\ell)$,

$$T = E_l e = E_l\left[\frac{1}{\cos\theta} - 1\right], \tag{4.5}$$

where

$$E_\ell = w_\ell E; \tag{4.6}$$

here E is Young's modulus for the liner material.

Equations (4.1)–(4.6) determine the equilibrium state (θ, H, T) for the cylindrical rock with its supporting liner as a function of the known mass of the rock and the bonding strength of the liner. The liner attachment angle θ can be eliminated from the system in favour of the tension T using (4.1) to give

$$T = E_l\left[\frac{T}{\sqrt{T^2 - B^2}} - 1\right],$$

$$2\pi B\left[R + H\frac{\sqrt{T^2 - B^2}}{B}\right] = Mg.$$

It is useful to use the total bonding force around the perimeter of the crack ($2\pi RB$) as a force scale and also scale lengths according to the rock radius,

$$T = BT', \quad Mg = (2\pi RB)W', \quad H = RH', \tag{4.7}$$

in terms of which the equations reduce to the dimensionless form,

$$T' = \frac{E_l}{B}\left[\frac{T'}{\sqrt{T'^2 - 1}} - 1\right], \tag{4.8}$$

$$H' = \frac{W' - 1}{\sqrt{T'^2 - 1}}. \tag{4.9}$$

https://doi.org/10.1017/S1446181123000172 Published online by Cambridge University Press

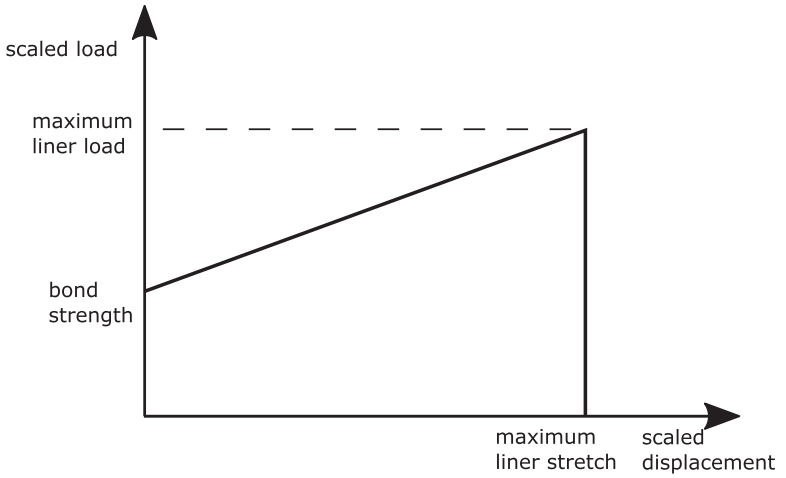

FIGURE 8. Loading versus displacement for the liner supported cylindrical rock.

Young's law, equation (4.8), can be solved exactly for $T'(E_l/B)$ using an algebraic package (the expression is complicated) and then the scaled rock displacement $H'(W')$ follows from (4.9).

One feature that comes out of the scaling is that significant movements (compared with the radius of the rock) will occur for rock masses of order $(2\pi RB)/g$, which is clear from (4.7), so that a doubling of the bonding strength will double the rock weight that can be supported. For $W' > 1$ the scaled displacement increases in direct proportion to $(W' - 1)$, with the proportionality factor dependent on the Young's modulus. This happens until the liner breaks. The generic behaviour is thus as shown in Figure 8, where the bonding strength and maximum stretch will vary with liner type and thickness, as will the Young's modulus and so the slope of the load–displacement curve. For the polyurethane liner case described in Table 1 it follows from (4.1) that the liner breaks when $\theta = \arcsin(1/8)$, which gives a maximum angle of 7 degrees before liner breakage. This curve should be compared with that shown earlier in Figure 3. The stress versus strain relationship for plastics is not quite linear; typically the material becomes stiffer at higher displacements, so that Figure 3 would be experimentally determined but the principles presented above hold.

In the above work, we envisaged a situation in which the tendency was for the rock to move perpendicularly to the wall face. In the tunnel situation, shear and hoop stresses can be set up in the surface of the wall, so that the liner may be subjected to longitudinal extension in the plane of the wall. Now if there is a crack in the wall face then the liner stretched across that crack will be locally strongly stretched and rupture is very likely. This occurs for example when paint covers a crack that then expands; the paint cracks.

In all the above work, we assumed no penetration of the liner into cracks. It should be remembered that any such penetration will have a major effect on the outcome.

https://doi.org/10.1017/S1446181123000172 Published online by Cambridge University Press

5. Conclusions

We first investigated the effectiveness of nonpenetrating TSLs in a lined tunnel subjected to a tensile perturbation due either to a seismic event or a mining disturbance. It was found that the shear and tensile stress in the liner and rock mass depend on the ratio E_1'/E_2' of the reduced elastic moduli. The effect of the liner on the stress distribution in the rock mass surrounding the tunnel is small, of order of magnitude of the thickness of the TSL, and is little influenced by the weak bonding factor λ. This is very different from the significant effect that penetration of liner material into fractures and cracks has on the stress distribution of the surrounding rock. The effect of the excavation on the liner tensile stress is large and occurs at zero order in ε through the factor E_1'/E_2'. To prevent build-up of tensile stress in the liner E_1'/E_2' should be kept small by choosing a liner with suitably small reduced elastic modulus E_1'. The zero-order term in the tensile stress in the liner does not depend on the weak bonding factor λ. It was found that the shear stress at the interface is small, of the order of magnitude of the thickness of the liner, and to this order it is independent of the weak bonding factor λ. The liner could therefore fail under tension but not under shear because the shear stress in the liner is only of order ε. In practice debonding between the liner and the rock will reduce tension in the liner and prevent liner failure under tension. The results show that in the liner tensile stress is more important than shear stress in supporting rocks and that debonding does not significantly affect the stress.

We next investigated local rock support. It was shown that support of loose rock movements is better achieved using a TSL with small Young's modulus but high rupture tensile strength. A doubling of the bonding strength of the liner to the rock will double the weight of rock that can be supported by the liner. Adhesive detachment from the tunnel wall is likely to occur before stress levels in the liner are sufficient to cause rupture because bonding strength is less than the shear and tensile strength of the liner.

Acknowledgments

D. P. Mason acknowledges financial support from the National Research Foundation, Pretoria, South Africa, under grant no. 96270. This paper is based on research done at the Twelfth Mathematics in Industry Study Group in South Africa held at the African Institute for Mathematical Sciences in 2015. The other members of the Study Group were M. Khalique, D. Aphane, Y. Bharath, A. H. Carrim, A. G. Fareo, A. B. Magan, V. Makibelo, W. Mhlanga, E. Mubai and Z. Ngcobo.

Recognition of the work of Graeme Hocking in South Africa

While the major contribution made by Graeme to the Mathematics in Industry Study Group (MISG) in Australia is widely acknowledged, less well known is the significant contribution he has made to the MISG in South Africa. Graeme has

https://doi.org/10.1017/S1446181123000172 Published online by Cambridge University Press

been a major contributor to the Study Group in South Africa since 2011. The venue for the meeting generally alternates between the University of the Witwatersrand in Johannesburg and the African Institute for Mathematical Sciences in Cape Town. In 2020 the MISG was held at the University of Zululand in KwaZulu-Natal near the industrial development zone at the Port of Richards Bay. Graeme's approach to problem-solving could be described as being no-nonsense and simple. Mathematical sophistication is only introduced as needed and the models he produces are minimal. The focus is clear and there is no excess. Typically Graeme moderates one problem but also contributes to the other problems at the meeting. He is willing to address any problem well outside his area of expertise, and his simple observations often redirect the focus. His advice and assistance are greatly appreciated by the graduate students and early-career academics. The Study Group moderated by Graeme always produced a Report for the Proceedings and Graeme made a major contribution to the writing of the Report. Through his contribution to the MISG Graeme has significantly advanced the development of mathematics in industry in South Africa.

References

[1] J. R. Barker, *Elasticity* (Kluwer Academic Publishers, Dordrecht, 1992).

[2] N. D. Fowkes, J. A. T. de Freitas and T. R. Stacey, "Crack repair using an elastic filler", *J. Mech. Phys. Solids* **56** (2008) 2749–2758; doi:10.1016/j.jmps.2008.06.001.

[3] D. P. Mason and T. R. Stacey, "Support to rock excavations provided by sprayed liners", *Int. J. Rock Mech. Min. Sci.* **45** (2008) 773–788; doi:10.1016/j.ijrmms.2007.09.001.

[4] T. R. Stacey, "Review of membrane support mechanisms, loading mechanisms, desired membrane performance and appropriate test methods", *J. South African Inst. Min. Metallurgy* **101** (2001) 343–351; https://hdl.handle.net/10520/AJA0038223X_2749.

[5] T. R. Stacey and X. Yu, "Investigations into mechanisms of rock support provided by sprayed liners", in: *Ground support in mining and underground construction* (eds. E. Villaescusa and Y. Potvin) (Taylor and Francis, London, 2004) 563–569.

[6] D. D. Tannant, "Thin spray-on liners for underground rock support", in: *Proc. 17th Int. Mining Congress and Exhibition of Turkey,* Balkema, 15–22 June, 2001 (Chamber of Mining Engineers of Turkey, Ankara, Turkey, 2001) 57–68; https://www.semanticscholar.org/paper/Thin-Spray-on-Liners-for-Underground-Rock-Support-Tannant/dcac8b181039d23fe7bd4cbae8a00aa102251fa7.